The Effect of Carrier in CO_2 Reforming of CH_4 to Syngas over Ni-based catalysts

Ho Joon Seo, Ung Il Kang [*], *and Eui Yeon Yu* [*]

Department of chemical engineering, Yosu National University, Yosu 550-747, Korea
[*]*Department of chemical engineering, Chonnam National University, Kwangju 500-757, Korea*

ABSTRACT : The activities of Ni(20wt%)/ La_2O_3, Ni(20wt%)/ $\gamma-Al_2O_3$, and Ni(20wt%)/ SiO_2 catalyst for CO_2 reforming of CH_4 were investigated in a fixed bed flow reactor under atmospheric condition. Catalyst characterization using XRD, TEM, SEM, BET analysis were also conducted. The catalytic activity of Ni(20wt%)/ La_2O_3 catalyst has relatively superior to that of Ni(20wt%)/ $\gamma-Al_2O_3$ and Ni(20wt%)/ SiO_2 catalyst. The good activity of Ni(20wt%)/ La_2O_3 catalyst seems to depend on reduced Ni° phases of NiO($\rightarrow$ Ni + O), $LaNiO_3$($\rightarrow$ Ni + La_2O_3), Ni crystalline phases, and decoration of Ni phases by lanthanum species is also an important factor. Ni(20wt%)/ $\gamma-Al_2O_3$ and Ni(20wt%)/ SiO_2 catalyst due to surface acidity resulted in the deposition of wisker type and encapsulate carbon on the surface of catalyst , but Ni(20wt%)/ La_2O_3 catalyst did not show carbon on the surface of catalyst up to 8.5hr reaction.
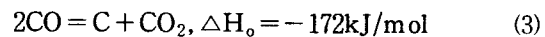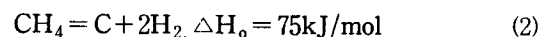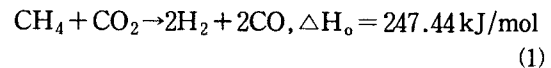
KEYWORDS : CO_2 reforming, CH_4, Ni, La_2O_3, $\gamma-Al_2O_3$, SiO_2, activity, carrier, catalyst

1. Introduction

Carbon dioxide is the main cause of the green house effect of earth, and in the future its emissions will increase continuously[1]. One method to reduce concentration of carbon dioxide on earth may be carbon dioxide reforming of methane to syngas using catalysts[2]. This would not make it possible only resolving the green house effect problem, but also reusing carbon resources for a feedstock of petrochemicals[3].

Moreover, the advantages of this method can be stated as follows : 1. produce lower H_2/CO ratio than conventional steam reforming. 2. be simpler process than the steam reforming. Carbon dioxide reforming is the endothermic reaction and it has the coke formation such as methane cracking and Buodouard reaction[4, 5].

$$CH_4 + CO_2 \rightarrow 2H_2 + 2CO, \triangle H_o = 247.44 kJ/mol \quad (1)$$
$$CH_4 = C + 2H_2, \triangle H_o = 75 kJ/mol \quad (2)$$
$$2CO = C + CO_2, \triangle H_o = -172 kJ/mol \quad (3)$$

Carbon dioxide reforming for producing syngas has researched since Gadalla, et al[6] reported the effect of support over Ni impregnated catalysts. Wang and Lu[7] reported that strong interaction between metal and the support made the catalyst more resistant to sintering and coking. Ruckenstein

and Hu[8] studied the role of support in CO_2 reforming of CH_4 to syngas over Ni catalysts, and their results showed that the sequence of CO yields was $Ni(13.6\%)/Al_2O_3 > Ni(13.6\%)/SiO_2 > Ni(13.6\%)/TiO_2$. Choudhary et al.[9] reported that $LaNiO_3$ perovskite showed high activity and selectivity in the oxidative conversion of methane to syngas. Moon et al.[10] researched the deposition of coke in carbon dioxide reforming of methane over nickel based catalysts, and they reported that the deposition carbon had a wiskerlike structure with a nickel particle at the end of the growing whiskers. Moreover, Rostrup-Nielsen et al.[11] and Kroll et al.[12] have suggested that carbon deposition be inevitable problem in carbon dioxide reforming of methane to syngas over Ni-based catalysts. However, the investigation of initial activity on acidic/basic nature of carrier employed was not reported. The purpose of the present study is to understand the initial activity of Ni-based carriers which lead to significantly different catalytic performance by conducting activity experiment with XRD, SEM, TEM, BET analysis.

2. Experimental

2.1. Catalyst preparation

The catalysts were prepared by impregnating La_2O_3(Aldrich chemicals) and $\gamma - Al_2O_3$ (Aldrich products), and SiO_2(Aldrich products) with an aqueous solution of $Ni(NO_3)_2.6H_2O$(Alfa chemicals). The obtained paste was completely dried at 120℃ in an oven for 24 hours, and then decomposed and calcined at 800℃ in air for 2hr.

2.2. Catalytic reaction

The catalytic reaction was carried out under atmospheric pressure in a fixed bed flow reactor. A quartz tube with 6mm inside diameter was used as

reactor. The catalyst powder of 0.020g weight was held on quartz wool. The CO_2/CH_4 molar ratio and contact time of reactant gas were 1 $molCO_2/molCH_4$ and 1.67×10^{-5} g-Cat.hr/ml, respectively. The reactor was maintained at a desired temperature with an accuracy of $\pm 1℃$ by a K-type thermocouple and PID controller. The catalyst was reduced in hydrogen with 180 ml/min rate at 500℃ for 3hr, followed by an increase in temperature to 800℃ at a rate of 20℃/min, and in hydrogen rate of 20ml/min. Effluent gas was analyzed with an on line gas chromatograph equipped with a porapak Q column. The yield of CO and H_2 is defined as follows :

$$H_2 \text{ yield(\%)} = \frac{\text{amount of } H_2 \text{ in products}}{2 \text{ x amount of } CH_4 \text{ in reactants}}$$

$$CO \text{ yield(\%)} = \frac{\text{amount of CO in products}}{\text{amount of } (CO_2 + CH_4) \text{ in reactants}}$$

2.3. X-ray powder diffraction, SEM, and TEM

X-ray powder diffraction was carried out on a Nicolet X-ray diffraction equipment at 20kV and 20mA using the $CuK\alpha(\lambda = 1.5405Å)$ radiation. Morphology of Ni-based catalysts was determined by using a JSM 5400(10^{-6}torr, 20kV), JEOL scanning electron microscope and a JEM-2000 FXII (10^{-5}Pa, 200kV), JEOL TEM.

2.4. BET Surface Area, Pore Size Distribution and Isotherm Plot

The surface area, pore size distribution, and N_2-isotherm plot were obtained by nitrogen adsorption using a Micromeritics ASAP 2000 instrument. The surface area and pore size distribution were calculated by the BET method and the BJH method, respectively.

The sample was degassed at 200℃ in high vacuum before measurements.

3. Results and Discussion

3.1. CO_2 reforming of CH_4 to Syngas

The conversion of CH_4 and CO_2 and the yield of CO and H_2 are plotted against the reaction time in the Fig.1-4, repectively. Fig. 1-4 clearly show that the conversion of CH_4 and CO_2 and the yield of CO and H_2 with reaction time depend on the carriers employed to prepare Ni-based catalysts. The activity of Ni(20wt%)/ La_2O_3 catalyst based on the yield of CO and H_2 has relatively superior to that of Ni(20wt%)/ $\gamma - Al_2O_3$ and Ni(20wt%)/ SiO_2 catalyst. However, Ni(20wt%)/ $\gamma - Al_2O_3$ and Ni(20wt%)/ SiO_2 catalyst have higher conversion of CH_4 than Ni(20wt%)/ La_2O_3 catalyst. The CO/H_2 molar ratios of the reduced Ni(20wt%)/ La_2O_3 and Ni(20wt%)/ $\gamma - Al_2O_3$, and Ni(20wt%)/ SiO_2 catalyst all have constant CO/H_2 mole ratio of 1 to 1, a theoretical stoichiometry ratio. These can be explained as a consequence of CH_4 cracking occurring over Ni(20wt%)/ $\gamma - Al_2O_3$ catalyst and Ni(20wt%)/ SiO_2 catalyst due to their acidic nature.
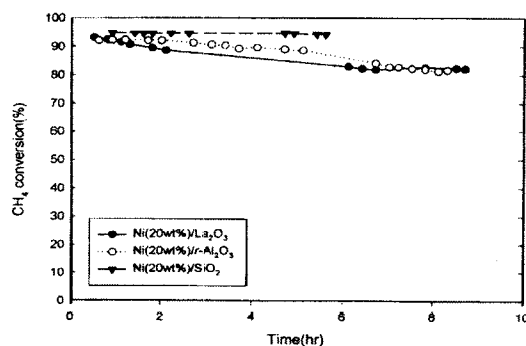

Fig. 1. CH_4 conversion vs. Time over Ni-based catalysts ; T=800°C, CO_2/CH_4 mol ratio = 1 : 1, W/F=1.67x10⁻⁵g-Cat.hr/ml
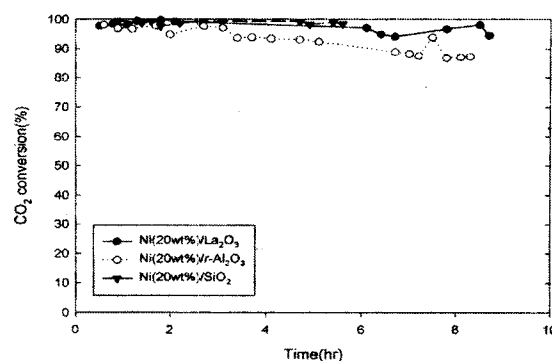

Fig. 2. CO_2 conversion vs. Time over Ni-based catalysts ; T=800°C, CO_2/CH_4 mol ratio = 1 : 1, W/F=1.67x10⁻⁵g-Cat.hr/ml
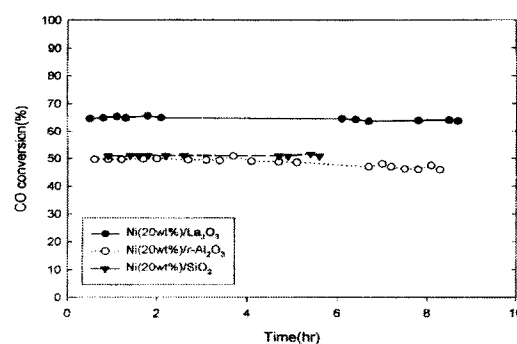

Fig. 3. CO yield vs. Time over Ni-based catalysts ; T=800°C, CO_2/CH_4 mol ratio = 1 : 1, W/F=1.67x10⁻⁵g-Cat.hr/ml
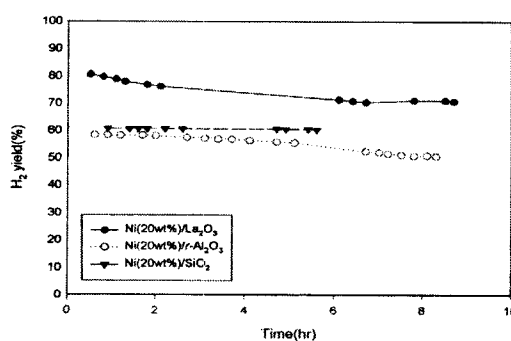

Fig. 4. H_2 yield vs. Time over Ni-based catalysts ; T=800°C, CO_2/CH_4 mol ratio = 1 : 1, W/F=1.67x10⁻⁵g-Cat.hr/ml

3.2. Catalyst characterization

The BET surface area, pore size distribution ,and N_2-isotherm plot of the Ni-based catalysts are summarized in Table 1 and Fig. 5-7, respectively.

Table 1. The BET surface area and pore size distribution of Ni-based catalysts.

Catalyst	BET surface area(m^2/g)	Pore size distribution(Å)
Ni(20wt%)/La₂O₃	10.0	< 100Å
Ni(20wt%)/ γ -Al₂O₃	69.2	20-400 Å
Ni(20wt%)/SiO₂	505.0	20-150 Å
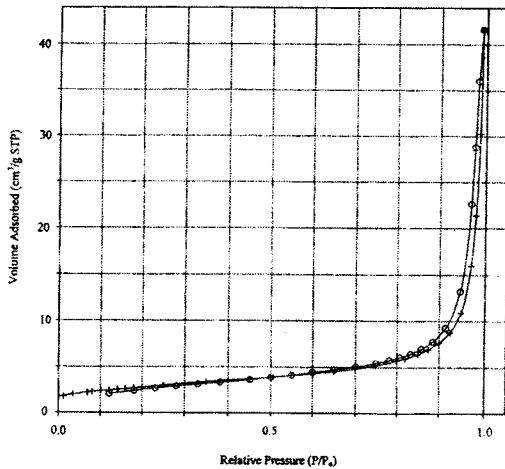
Fig. 5. N₂-Isotherm plot of Ni(20wt%)/La₂O₃ catalyst. +, adsorption; o, desorption
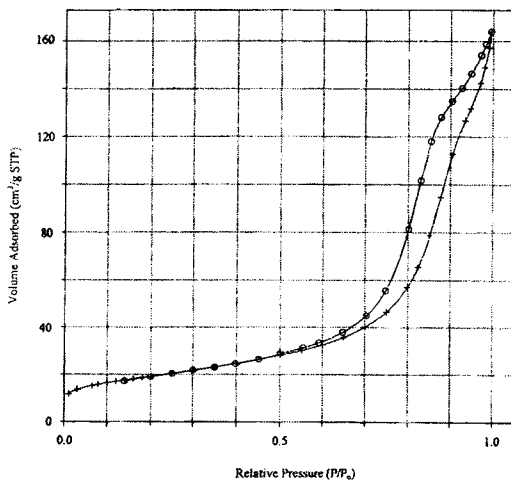

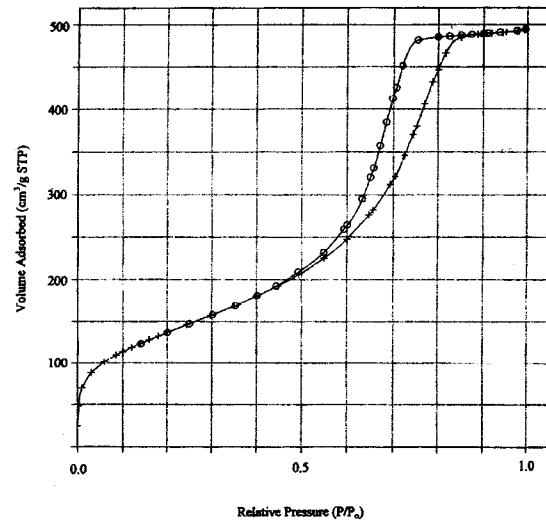Fig. 6. N₂-Isotherm plot of Ni(20wt%)/γ-Al₂O₃ catalyst. +, adsorption; o, desorption

Fig. 7. N₂-Isotherm plot of Ni(20wt%)/SiO₂ catalyst. +, adsorption; o, desorption

Table 1 shows BET surface area and pore size distribution of Ni(20wt%)/ La_2O_3, Ni(20wt%)/ $\gamma - Al_2O_3$, and Ni(20wt%)/ SiO_2 catalyst. The pore size distribution shows that Ni(20wt%)/ La_2O_3 have both micropores and mesopores, but Ni(20wt%)/ $\gamma - Al_2O_3$ and Ni(20wt%)/ SiO_2 catalyst have the only mesopores. The BET surface area of catalysts was Ni(20wt%) / SiO_2> Ni(20wt%) / $\gamma - Al_2O_3$>Ni(20wt%)/ La_2O_3. The Ni(20wt%) / La_2O_3 catalyst is classified as type V isotherm according to Brunaur, Deming, and Teller, but Ni(20wt%)/ $\gamma - Al_2O_3$ and Ni(20wt%)/ SiO_2 catalyst are classified as type IV isotherm with outstanding hysteresis. These show that physical properties of Ni(20wt%)/ La_2O_3 catalyst is different from Ni(20wt%)/ $\gamma - Al_2O_3$ and Ni(20wt%)/ SiO_2 catalyst. Fig. 8 shows the XRD spectra of Ni(20wt%) / La_2O_3 catalyst before and after reaction. XRD spectra of Ni(20wt%)/ La_2O_3 catalyst show that Ni-La₂O₃ crystalline phases before reaction turn into NiO(1 1 1), LaNiO₃(2 0 2), Ni(2 0 0)

crystalline phases by uniform diffusion of Ni particles into LaO_x lattice after reaction. The Ni^o phases of $NiO(\rightarrow Ni + O)$, $LaNiO_3(\rightarrow Ni + La_2O_3)$, Ni crystalline phases were reduced by syngas, and then take part in the CO_2 reforming, and they seem to be reponsible for the high activity of $Ni(20wt\%)/ La_2O_3$ catalyst. Moreover, the perovskite, $LaNiO_3$ at $2\theta =$ $32.3°, 47.0°, 58.4°, 69.7°$ before reaction turn into La_2O_3 and Ni^o after reaction, and then Ni^o continuously participate in the CO_2 reforming. Ni^o phases at $2\theta = 44.5°, 76.4°$ also contribute to enhance the activity of $Ni(20wt\%)/ La_2O_3$ catalyst. TEM micrographs of $Ni(20wt\%)/ La_2O_3$ catalyst before and after reduction is represented in Fig. 9. It clearly showed lanthanum species to cover a portion of the surface of Ni particles. This can explain that the good activity of $Ni(20wt\%)/ La_2O_3$ catalyst is related to decoration of the Ni phases by lanthanum species remained on the surface of Ni crystalline phases after reduction. Scanning electron micrographs(SEM) of $Ni(20wt\%)/ La_2O_3$ catalyst before and after reaction are represented in Fig. 10. Fig. 11 shows SEM photographs of $Ni(20wt\%)/$ $\gamma -Al_2O_3$ and $Ni(20wt\%)/ SiO_2$ catalyst after reaction. Morphology of $Ni(20wt\%)/La_2O_3$ catalyst before reaction is shown to have smaller particles uniformly distributed on the surface of catalyst, but after reaction it seems to be diffused of Ni in the matrix of La_2O_3 or/and to be coagulated by interaction between NiO and La_2O_3 by sintering. $Ni(20wt\%)/ La_2O_3$ catalyst do not also show carbon on the surface of catalyst up to 8.5 hr. Morphology of $Ni(20wt\%)/ \gamma -Al_2O_3$ and $Ni(20wt\%)/ SiO_2$ catalyst after reaction shows that

both wisker and encapsulate forms of carbon are present on the catalyst surface. This could be suggested that $Ni(20wt\%)/ La_2O_3$ catalyst with basic carrier has the more resistance to carbon deposition of catalyst than $Ni(20wt\%)/ \gamma -Al_2O_3$ and $Ni(20wt\%)/ SiO_2$ catalyst with acidic carrier.

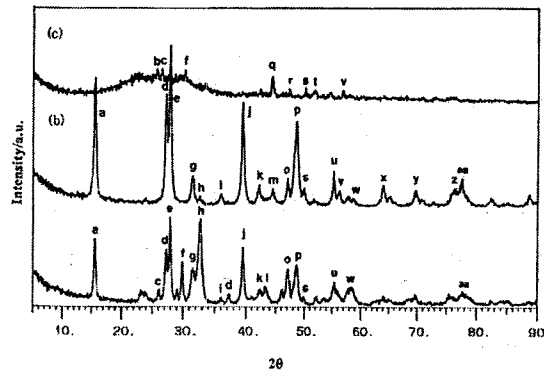
Fig. 8. XRD pattern of $Ni(20wt\%)/La_2O_3$ catalyst. (a) fresh catalyst ; (b) after reduction; (c) after reaction

: a, LaNi(0 2 0); b, La₂O₃(1 0 0); c, LaNi(0 2 1); d, La₂O₃(0 0 2); e, La₂O₃ (1 0 1); f, NiO(1 1 1); g, LaNi(1 1 1); h, LaNiO₃(1 0 0); i, La₂Ni₃(0 4 0); j, LaNi(1 3 1); k, La₂O₃(0 0 3); l, NiO(2 0 0); m, Ni(1 1 1); o, LaNiO₃(2 0 0); p, LaNi₃(0 2 7); q, La₂O₃(1 1 0); r, LaNiO₃(2 0 2); s, La₂O₃(1 0 3); t, Ni (2 0 0); u, LaNi(0 6 1); v, La₂Ni₃(0 6 0); w, LaNiO₃(2 1 1); x, LaNi(2 0 2); y, LaNiO₃(0 2 4); z, Ni(2 2 0); aa, LaNi(3 3 0)
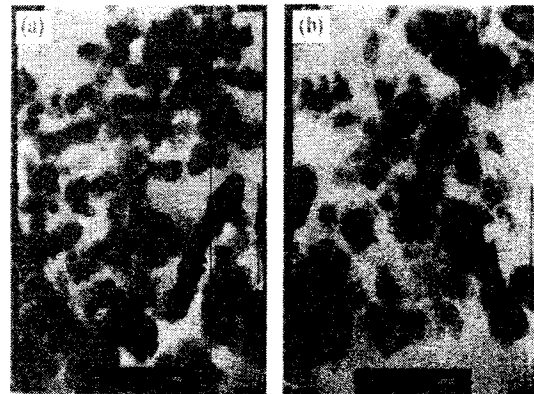

Fig. 9. TEM photographs Ni(20wt%)/La₂O₃ catalyst.
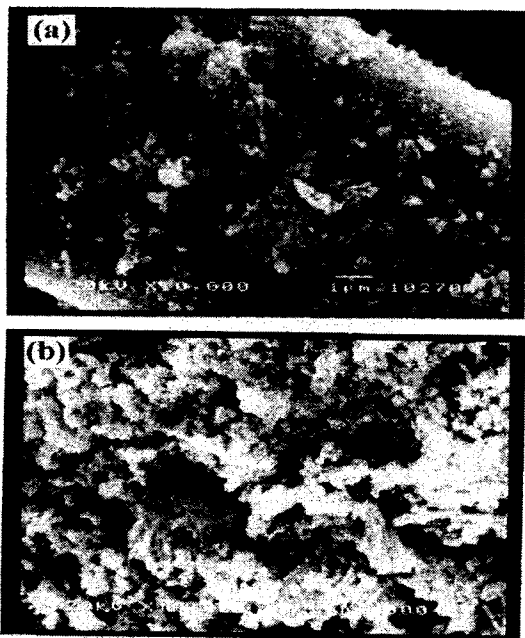(a) before reduction; (b) after reduction

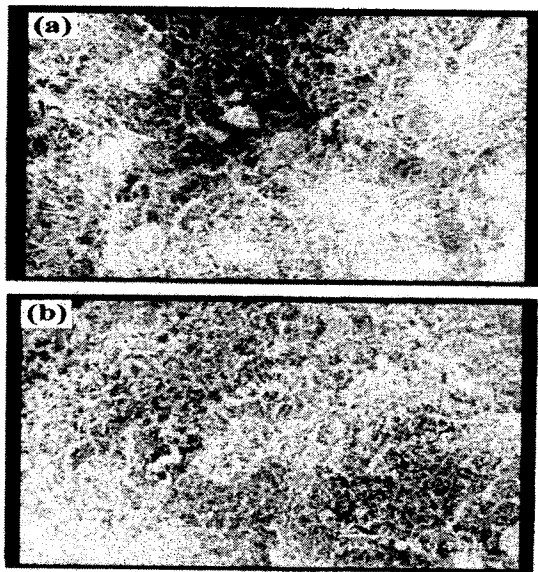Fig. 10. Scanning electron micrographs of Ni(20wt%)/ La_2O_3 catalyst. (a) before reaction; (b) after reaction

Fig. 11. Scanning electron micrographs of Ni(20wt%)/γ-Al_2O_3 and Ni(20wt%)/SiO_2 catalyst after reaction.
(a) Ni(20wt%)/γ-Al_2O_3; (b) Ni(20wt%)/SiO_2

4. Conclusions

CO_2 reforming of CH_4 to syngas over Ni-based catalysts in a fixed bed flow reactor at atmospheric condition is obtained as follows.

1. The activity of Ni(20wt%)/ La_2O_3 catalyst has relatively superior to that of Ni(20wt%)/ γ $-Al_2O_3$ and Ni(20wt%)/ SiO_2 catalyst with time on-stream.

2. The good activity of Ni(20wt%)/ La_2O_3 catalyst may depend on reduced Ni° phases of NiO(→ Ni + O), LaNiO3(→ Ni + La2O3), Ni crystalline phases, and decoration of the Ni phases with lanthanum species may also play a role.

3. The carbon deposition on the surface of catalyst is affected by acidic/basic nature of the carrier employed.

References

1. Moon, K. I., Kim, C.H. Choi, J. S., Lee, S. H., Kim, Y. G. and Lee, J. S. : *HWAHK KONGHAK* 35, 883(1997).

2. Richardson, J. T. and Paripatyadar, S. A. : *Appl. Catal.* 61, 293(1990).

3. Gadalla, A. M. and Sommer, M. E. : *J. Am. Cerma. Soc.* 72, 683(1990).

4. J. B. Claridge, J. B., Green, M. L. H., Tsang, S.C.T., York, A.P.E. Ashcroft, A.T. and Battle, P. D. : *Catal. Letters* 22, 299(1993).

5. Seo, H. J. and Yu, E. Y. : *J. of Ind. & Eng. Chemistry* 3, 85(1997).

6. Gadalla, A.M. and Bower, B. : *Chem. Eng. Sci.* 43, 3049(1998).

7. Wang, S. and Lu, G.Q.M. : Appl. Catal. B ; Environmental 16, 269(1988).

8. Ruckenstein, E. and Hu, Y.H. : *J. Catal.* 162, 236(1996).

9. Choudhary, V.R., Uphade, B.S., and Belhekar, A.A. : *J. Catal.* 163, 312(1996).

10. Moon, K. I., Kim, C. H. Choi, J. S., Lee, S. H., Kim, Y. G. and Lee, J. S. : *HWAHK KONGHAK* 35, 890(1997).

11. J. R. Rostrup-Nielsen, J. R. and Hansen, J-H.B. : *J. of Catal.* 144, 38(1993).

12. Kroll, V.C.H., Swaan, H.M. and Mirodatos, C. : *J. of Catal.* 161, 409(1996).